Fungal Composition and Diversity of the Tobacco Leaf Phyllosphere during Curing of Leaves

Qian-Li Chen
  Guizhou University

Lin Cai
  Southwest University

Hancheng Wang (✉ xiaobaiyang126@hotmail.com)
  Guizhou Academy of tobacco science   https://orcid.org/0000-0001-7423-7121

Liu-Ti Cai
  Guizhou Academy of tobacco science

Paul Goodwin
  University of Guelph

Jun Ma
  Qianxinan branch of guizhou tobacco company

Feng Wang
  Guizhou adademy of tobacco science

Zhong Li
  Guizhou University

Abstract

Background: *Rhizopus oryzae* causes tobacco pole rot in China during tobacco flue-curing. Flue-curing is a post-harvest process done to prepare tobacco leaves and involves three different stages: the yellowing stage has the lowest temperatures and highest humidity, then the color-fixing stage has higher temperatures and medium humidity, and finally the stem-drying stage has the highest temperatures and lowest humidity.

Results: In this study, fungal culturing and IonS5[TM]XL high-throughput sequencing techniques were used to reveal the fungal community of the petioles and lamina of tobacco leaves infected with pole rot during flue-curing. A total of 108 fungal isolates belonging to 5 genera and 10 species were isolated on media. The most common fungi isolated was *R. oryzae*, most often found equally on petioles and laminas in the color-fixing stage, followed by saprotrophs, mostly *Aspergillus fumigatus* and *Aspergillus flavus*. High-throughput sequencing revealed saprotrophs, *Alternaria* being the most abundant genus, followed by *Phoma*, *Cercospora* and *Aspergillus*, whereas *Rhizopus* was the tenth most abundant genus, which was mostly found on petioles at the yellowing stage. Both culturable fungal diversity and fungal sequence diversity was higher at stem-drying stage than the yellowing and color-fixing stages, and diversity was higher with leaf lamina than petioles revealing that the changes in fungal composition and diversity during the curing process were similar with both methods.

Conclusions: A better understanding of the saprotrophic fungi during curing of leaves with pole rot could result in the identification of highly competitive saproptrophs that may act as potential biocontrol agents of tobacco pole rot.

1. Introduction

Tobacco *(Nicotiana tabacum* L.) is a leafy, annual, solanaceous plant grown commercially for its leaves. It is one of the most widely grown commercial non-food crop in the world [1]. The leaves of tobacco are normally first harvested in commercial field and then flue-cured in a baking barn [2]. The purpose of flue-curing is to produce dried leaves of suitable physical properties and chemical composition [3, 4]. Leaf curing typically goes three stages, the yellowing stage with temperatures of <45 °C and relative humidity over 75%, color-fixing stage with temperatures of 45-55 °C and relative humidity over 35%, and stem-drying stage with temperatures of 55-70 °C and relative humidity under 30% [5]. During the curing process, many post-harvest pathogens can occur causing lesions and rots of tobacco leaves, including *Erwinia carotovora* and *Bacillus polymyxa* [6], *Aspergillus* and *Penicillium*, and *Alternaria* and *Cladosporium* [7].

Recently, the fungus *Rhizopus oryzae* has been associated with tobacco pole rot in China [8, 9]. The fungus grows from the basal part of the midrib of the sessile leaf and spreads on the lamina initially forming white cottony mycelia fading from white to black as spores are produced. Under high humidity and warm temperatures during the leaf yellowing stage, the fungus can rot leaves within the first 48 h [10]. Spores of the pathogen remain viable during the high temperatures of the stem drying stage and thus survive from year to year in a flue-curing barn [11]. In the last five years, tobacco pole rot was the most severe and most common post-harvest disease in flue-cured tobacco in China with losses reaching up to 100% [12].

Plant diseases usually change the microbial phyllosphere community structure [13, 14] (Luo et al. 2019, Raza et al. 2019). OTU biodiversity analysis of phyllosphere microbiome has been reported for during several tobacco diseases, including black shank, brown spot and pole rot of tobacco [15-17]. However, the study of Chen et al. on pole rot only examined the microbial phyllosphere on tobacco tissues sampled at the end of stem-drying stage, and thus it is unknown if the same changes occur during the curing process where tobacco pole rot occurs.

Many methods have been used to study microbial composition and diversity. Cultural methods are normally easy to perform but are time consuming and can only detect <1% of microorganisms [18, 19]. Culture-independent methods, particularly high-throughput sequencing, are more sensitive and reliable for the identification of culturable and non-readily culturable microorganisms [20]. Chen et al. (2019) found the fungal community composition, relative abundance and dominant fungal taxon of each sample that with different pole rot level were all different. When at genus level for sample leaf lamina, the dominant genus was *Aspergillus*, *Myrothecium, Rhodotorula* and *Gibberella*. For sample leaf petioles, dominant genus was *Aspergillus* and *Alternaria*.

It is important to characterize the fungal communities of leaf phyllosphere microorganisms to understand if pole rot affects them during the curing process. In a curing chamber, the temperature is normally lower and relative humidity normally higher at greater

heights. Therefore, tobacco leaf lamina and petioles at the three different curing height positions during the three curing stages were selected. The fungal composition and diversity of the tobacco leaf phyllosphere was analyzed both by cultural and high-throughput sequencing techniques. The results help reveal changes in the fungi associated with leaves having pole rot during curing, providing potential candidates for biocontrol agents of tobacco pole rot.

2. Materials And Methods

2.1 Environmental conditions

Air relative humidity was measured by a hygroscope. Air, lamina and petiole temperatures were measured by a baking thermometer. Leaf lamina and petiole wetness was measured by a hygrometer recorder, and wind speed was measured by an anemoscope. Measurements were taken at 2.5 m, 1.75 m and 1 m above ground level in the curing chamber at 42, 94 and 140 hours post-harvest (hph).

2.2 Sampling sites and sampling strategy

In August 2018 in Guizhou province (26°36'N, 107°59'E) of China, one curing barn with pole rot disease was chosen for sampling. Leaves were collected from three different curing positions at 2.5 m (upper), 1.75 m (middle) and 1.0 m (lower) from ground level. Leaves of *N. tabacum* cultivar Yunyan 87 were harvested on 7th August from a commercial field and placed in a curing chamber starting 9th August. At yellowing (42 hph), color-fixing (94 hph) and stem-drying (140 hph) stages, 10 g of tobacco leaves at the upper, middle and lower curing positions were randomly sampled, and the petioles and leaf laminas were then separated. For coding samples, the letter A was used for petioles and B for lamina, which was followed by the number 1 for yellowing stage, 2 for color-fixing stage and 3 for stem-drying stage, and then finally followed by 1 for upper, 2 for middle and 3 for lower height positions. For example, A31 was petiole during the stem drying stage at the upper chamber position. Three biological repeats were conducted (Table 1). Leaf samples were immediately taken to the laboratory of Guizhou Academy of Tobacco Science at 4 °C prior to culturing or -80 °C prior to high-throughput sequencing.

2.3 Isolation and molecular identification of leaf culturable fungi

Culturable fungi were isolated by using the tissue separation method [21]. Fungi were isolated on potato dextrose agar (PDA) containing 20 g glucose, 6 g potato powder and 20 g agar per liter of distilled water, or alkyl ester agar (AEA) containing 5 g yeast extract, 6 g $NaNO_3$, 1.5 g KH_2PO_4, 0.5 g KCl, 0.25 g $MgSO_4$, 20 ml glycerin, and 20 g agar per liter of distilled water [22]

Necrotic petiole and lamina tissue pieces (5 mm × 5 mm) were stertilized with 70% ethanol for 30 s, then with 10% sodium hypochlorite (NaOCl) for 2 min, air dried and placed on both PDA and AEA plates. After 5 days at 28 °C in the dark, hypha was transferred a new plate for purification. Fungi with different pigments, growth rates and morphologies were isolated from the plates. All purified fungi were stored on PDA slants at 4 °C.

For molecular identification of each culturable isolate, the rDNA internal transcribed spacer region (ITS) was amplified and sequenced. PCR-amplification was conducted using primers ITS1F (5 '-CTTGGTCATTTAGAGGAAGTAA-3 ') and ITS4 (5' - TCCTCCGCTTATTGATATGC-3'). The amplified fragments were sequenced, and used as a query in a BLASTN search of the NCBI nr database (http://www.ncbi.nlm.nih.gov/). Matches with identity values higher than 98% were used for the identification of the isolates.

2.4 ITS amplification and High-throughput sequencing

DNA of symptomatic petioles and laminas were separately extracted using FastDNA®Spin kit according to the manufacturer's instructions (MP Biomedicals, Santa Ana, CA, USA), and eluted in a final volume of 80 μL. Quantity and quality of the DNA solution were assessed by agarose gel electrophoresis, and concentration and purity were assessed by NanoDrop ND-2000 (Thermo Fisher Scientific, Waltham, MA, USA).

Full-length ITS rDNA of the pure fungal isolates was PCR-amplified using primers ITS5 (5'-GGAAGTAAAAGTCGTAACAAGG-3') and ITS2 (5'-GCTGCGTTCTTCATCGATGC-3'). PCRs were carried out in 30 μL reactions in triplicate, with each reaction tube containing 3

μL of each primer (2 μM), 2 μL of template DNA (1 ng/μL), and 2 × Phusion High-Fidelity PCR Master Mix with GC Buffer 15 μL. The following PCR condition was used: 98 °C for 1min, 98 °C 10 sec, 50 °C 30 sec and 72 °C 30 sec for 30 cycles, and a final extension of 72 °C for 50 min. PCR products were subjected to electrophoresis on a 2% agarose gel subsequently, and the targeted fragment size (ITS 306 bp) was purified with Gene JET (Thermo Fisher Scientific, Waltham, MA, USA). Leaf fungal DNA samples were sequenced at the Novogene Bioinformatics Technology Co., Tianjin, China using 250 bp paired-end sequencing with an Ion S5™ XL platform (Thermo Fisher Scientific, Waltham, MA, USA).

2.5 High-throughput sequencing and statistical analysis

High-throughput sequencing was performed using the Ion S5™ XL platform at Novogene Bioinformatics Technology Co, Beijing, China. The script from Novogene Corporation was used for clipping barcode and primer sequences by Cutadapt (V1.9.1, http://cutadapt.readthedocs.io/en/stable/). The UPARSE pipeline (v7.0.1001, http://www.drive5.com/uparse/) was used to analyze operational taxonomic units (OTUs) and other biological information of the sequences obtained from each sample. The similarity was set to 97%. Species annotation was added to the representative OTU sequences. The community composition of each sample was counted at the kingdom, phylum, class, order, family, genus and species levels by Unit (v7.2, https://unite.ut.ee/). Spearman's correlation analysis was used to determine the relationships between environmental factor and the relative abundances of keystone species (Clarke K R. 2010). After obtaining the sequencing result and calculation of OTUs matrix, Qiime (V. 1.9.1) was used for full-sample similarity comparison to analyze the alpha-diversity and calculate the observed-species, Chao1, Shannon, Simpson, ACE, and Good's-coverage indices. R software (Version 2.15.3) was used to draw a dilution curve, rank abundance curve, and species accumulation. Beta diversity on both weighted and unweighted unifrac were calculated by Qiime software (Version1.7.0). Principal Component Analysis (PCA) was displayed by WGCNA packages and ggplot2 package in R software (Version 1.9.1). Each OTU was assigned to a functional guild using the FUNGuild database.

3. Results

3.1 Environmental conditions

During the curing process where tobacco pole rot occurs in the curing chamber, relative humidity declined from 84-91.5% to 8.5-22%, lamina wetness declined from 63-67% to 4-14%, and petiole wetness declined from 73-78% to 5-20% (Table 1). In contrast, air temperature increased from 37-38 to 67-68 °C, and lamina temperature increased from 35-36 to 65-66 °C. Wind speed was only higher during the color-fixing stage. This shows that tissues are drying with increasing temperatures over time. Position in the chamber was correlated with relative humidity, decreasing at progressively lower positions from 91.5 to 84%, 73 to 57%, and 22 to 8.5% in the yellowing, color-fixing and stem-drying curing stages, respectively. In contrast, air temperature increased at progressively lower positions from 37 to 38 °C, 47 to 48 °C, and 67 to 68 °C in the yellowing, color-fixing and stem-drying curing stages, respectively.

3.2 Culture-based fungal diversity and abundance

A total of 108 fungal isolates belonging to 5 genera and 10 species were obtained by tissue isolation method (Table 2). More species were isolated on PDA (*R. oryzae*, *E. thailandicum*, *D. ovalispora*, *A. oryzae*, *A. fumigatus*, *A. flavus*, *A. aflatoxiformans*, *A. alternata*) than on AEA (*R. oryzae*, *E. sorghinum*, *C. tenuissimum*, *A. fumigatus*, *A. flavus*). The most abundant species was *R. oryzae* comprising 33 of the 54 isolates on PDA and 35 of the 54 isolates on AEA, followed by *A. flavus* with 10 of the isolates on PDA and 9 of the isolates on AEA and *A. fumigatus* with 6 isolates on PDA and 6 on AEA. The rarest species were *E. thailandicum*, *D. ovalispora*, *A. oryzae*, *A. aflatoxiformans*, *A. alternata, E. sorghinum* and *C. tenuissimum*.

When analyzed for curing stage combining lamina and petiole samples, diversity was highest during the color-fixing curing stage with 10 species, and lowest at the stem-drying curing stage with 2 species (Table 2). The relative abundance (% of isolates of a species out of the total number of isolates) during the yellowing curing stage showed that *R. oryzae* was most abundant (12.04% on AEA and 13.89% on PDA), during the color-fixing stage showed that *A. flavus* (5.56% on AEA and 7.41% on PDA) and *A. fumigatus* (3.70% on AEA and 3.70% on PDA) were most abundant, and during the stem drying stage showed that *R. oryzae* (16.67% on AEA and 15.74% on PDA) was most abundant. Isolates of *E. sorghinum* (1.85% on AEA and 0% on PDA), *C. tenuissimum* (1.85% on AEA

and 0% on PDA), *E. thailandicum* (0% on AEA and 0.93% on PDA), *D. ovalispora* (0.93% on AEA and 0% on PDA) and *A. oryzae* (0% on AEA and 0.93% on PDA) were only found during the color-fixing curing stage.

When analyzed for tissue type combining curing stages, diversity was highest for lamina with 9 species compared to petioles with 5 species (Table 2). The relative abundance showed that *A. flavus* (4.63% on AEA and 5.56% on PDA) and *A. fumigatus* (3.70% on AEA and 2.78% on PDA) were higher in petiole, whereas *R. oryzae* was highest in both petiole (14.81% on AEA and 15.74% on PDA) and lamina (17.59% on AEA and 14.81% on PDA).

3.3 Sequence-based fungal diversity

There was a total of 4,373,082 high-quality sequences across the 27 petiole and 27 lamina samples. A total of 2,238 OTUs at ≥ 97% nt identity were obtained from the 54 samples after the removal of low quality, chimeric and rare sequences resulting in an average number of sequences per sample of 80,983. When the number of sequences reached approximately 40,000, the rarefaction curves for all 54 samples revealed that they approached the plateau phase (Fig.1), suggesting that there was sufficient sequence coverage to describe the fungal composition.

Comparing between curing stages showed that the total number of OTUs progressively increased with significantly more OTUs at the stem-drying stage than the yellowing stage (Table 3). For petioles, the number OTUs increased between curing stages, with significant differences between the yellowing stage and the stem-drying stage. For leaf laminas, the number OTUs increased between curing stages, with significant differences between the yellowing stage and the stem-drying stage.

Comparing between positions showed that during the yellowing stage, the number of OTUs for petioles were not significantly different, but the number of OTUs for leaf laminas were significantly greater in the upper position than the lower position (Table 3). During the color-fixing stage, there were significantly higher numbers of OTUs at the middle compared to the upper position for petioles, but no significant differences for leaf lamina. During the stem-drying stage, no significant differences were found for petioles based on position, but there were significantly lower OTU numbers in the upper and middle positions compared to the lower position for leaf lamina (Table 3).

OTUs on petioles at the stem drying stage and on lamina at the stem drying stage, regardless of position, had highest diversity based on the average Shannon, Simpson, Chao1 and ACE values (Table 3). The next highest diversity of the OTUs was at the color-fixing stage for both petiole and lamina samples, regardless of position based on the average Shannon, Simpson, Chao1 and ACE values. The lowest diversity index values were found for OTUs at the yellowing stage for both petiole and lamina samples, regardless of position based on all four diversity indices.

3.4 Taxonomic composition of the OTUs

The distribution of phyla for the OTUs showed that 88.29% of the clean sequence reads could be classified in the Ascomycota, Basidiomycota, Mucoromycota, Glomeromycota, Mortierellomycota, Blastocladiomycota, Olpidiomycota and Chytridiomycota. Members of the other phyla were unassigned, and were likely not true fungi (Fig 2). The fungal communities were dominated by the Ascomycota (47.36%), followed by the Basidiomycota (5.88%) and the Mucoromycota (0.60%). Combined together, the Glomeromycota, Mortierellomycota, Blastocladiomycota, Olpidiomycota and Chytridiomycota comprised only 0.01% of the reads.

Combining position and tissue type, the average number of reads per curing stage for the Ascomycota was 56.10%, 47.17%, 38.80% in the yellowing stage, color-fixing stage and stem-drying stage, respectively, indicating a decline as curing occurred. In contrast, the relative abundance for all samples for the Basidomycota was 4.12%, 7.11%, 6.41% in the yellowing stage, color-fixing stage and stem-drying stage, respectively, indicating a peak in the color-fixing stage. The relative abundance for all samples for the Mucoromycota was 1.01%, 0.15%, 0.65% in the yellowing stage, color-fixing stage and stem-drying stage, respectively, indicating a decline during curing. Combining position and curing stage, the relative abundance of samples based on tissue type showed that Ascomycota were 46.68% and 48.03%, Basidiomycota were 5.57% and 6.18%, Mucoromycota were 0.96% and 0.24% for petioles and lamina, respectively, indicating that there was no significant difference based on tissue type.

A total of 35.97% of the OTUs could be classified at the genus level. The 30 most common genera are shown in Fig 3. Among those, the 10 highest number of reads were for *Alternaria*, *Phoma*, *Cercospora*, *Aspergillus*, *Cladosporium*, *Symmetrospora*, *Boeremia*,

Stagonosporopsis, *Epicoccum* and *Hannaella*. However, *Rhizopus*, which would include the pole rot pathogen, *R. oryzae*, had only 0.60% of the reads. Thus, the reads were dominated by OTUs for saprophytic, rather than pathogenic fungi.

A maximum likelihood tree of the 100 most abundant fungal genera showed that the most dominant fungi were in the Ascomycota, followed by Basidiomycota, and the least common fungi were in the Mucoromycota (Fig 4). For the Ascomycota, the dominant genera were *Alternaria*, *Aspergillus*, *Cerospora*, *Cladosporium*, *Phoma*, *Boeremia*, *Golovinomyces*, *Stagonosporopsis* and *Epicoccum.* For the Basidiomycota, the dominant genera were *Symmetrospora*, *Hannaella*, *Golubevia* and *Rhodotorula*. For the Mucoromycota, the dominant genera was *Rhizopus*, which would include *R. oryzae*.

The abundance of the top 10 genera varied considerably among the samples (Table 4). *Alternaria* was the highest at B21 followed by A31 and A21, indicating that it was more common in the upper position and somewhat more common in petiole than the lamina. *Phoma* was the highest at B13 followed by A12 and B11, indicating that it was also favored during the leaf yellowing stage. *Boeremia* was most common in B1, followed by B23 and B13, indicating that it has most abundant for lamina, curing stage or position. *Cercospora* was most abundant B31 followed by B22 and A22, indicating that it was more common in the upper position and somewhat more common in petiole than the lamina. *Aspergillus* was most common in A32, B32 and A33, indicating that the stem-drying stage at the middle and lower positions favored it. *Rhizopus* was the most dominant genus in A11, B32 and A31, indicating it was most common in petioles during the yellowing stage.

3.5 The relationship to environmental parameters

Spearman correlation analysis of the most abundant genera was made between air temperature, relative humidity, curing stage, position, wind speed and wetness of leaf and petiole (Fig. 5). Air temperature significantly affected the abundance of *Golovinomyces.* Relative humidity significantly affected the abundance of *Alternaria*, *Phoma*, *Trichoderma*, *Leptosphaerulina*, *Gibellulopsis*, and *Candida*. Curing stage significantly affected the abundance of *Golovinomyces*, *Golubevia*, *Strelitziana*, *Dioszegia* and *Pestalotiopsis*. Sample position significantly affected the abundance of *Alternaria*, *Aspergillus*, *Rhizopus* and *Leptosphaerulina*. Wind speed significantly affected the abundance of *Golovinomyces*, *Golubevia*, *Septoriella*, *Strelitziana*, *Dioszegia* and *Pestalotiopsis*. Wetness of leaf and petiole significantly affected the abundance of *Alternaria*, *Stagonosporopsis*, *Trichoderma*, *Leptosphaerulina*, *Gibellulopsis* and *Candida*. In general, *Alternaria*, *Phoma*, *Golovinomyces*, *Strelitziana*, *Leptosphaerulina* and *Pestalotiopsis* were the genera affected by the most environmental factors. *Rhizopus*, which would include the pole rot pathogen *R. oryzae* was only significantly affected by position.

3.6 Spatial distribution of microbial communities

PCA showed that the first two PCs accounted for 4.4% and 8.12% of the total variance in the fungal communities of the 18 sample groups (Fig. 6). All of the fungal communities overlapped with each other, except for three distinctive fungal communities, which were for the upper petiole samples at the yellowing stage (B11), the lower lamina samples at stem-drying stage (B33) and the lower petiole samples (A33).

3.7 Functional guilds analysis

FUNGuild database was used to classify the fungi in present study by ecological guild (Fig. 7). Members of the pathotroph-saprotroph-symbiotroph were the most common at 13.68% of sequences, pathotroph was the second most common at 13.37% of sequences, pathotroph-saprotroph was the third most common at 10.56% of sequences, saprotroph was the fourth most common at 6.81% of sequences, pathotroph-symbiotroph was the fifth most common at 4.22% of sequences, and the least common were symbiotroph, saprotroph-symbiotroph and pathogen-saprotroph-symbiotroph at 0.20, 0.10 and <0.10% of the sequences, respectively. However, the unassigned sequences was the largest group at 51.77%. For the average based on sample type, pathotroph-saprotroph-symbiotroph was the most abundant in petioles and lamina. For the average based on curing stage, pathotroph was most abundant in leaf yellowing, color fixing and stem drying stages, respectively.

4. Discussion

The diversity and function of tobacco leaf phyllosphere fungi were previously studied by culture-dependent methods [23], but the application of next generation sequencing technology to examine microbial populations in tobacco has revealed a much greater

diversity of fungi [24]. In present study, a higher fungal diversity on tobacco leaves in a tobacco curing barn where tobacco pole rot occurred was found using high-throughput sequencing than a culture-dependent approach.

A comparison of cultivable fungal populations obtained on two different media (PDA and AEA) did not show any statistical differences, indicating that the media composition did not affect the detectable cultivable fungus strains. Only ten culturable fungal genera were obtained in the present study, showing the limitations of cultivation-dependent methods. Microorganisms recovered from the environment by traditional culturing methods are rarely abundant in terms of their actual numbers or their functions in the environment, and it is estimated that less than 1% of microorganisms are readily culturable [25-27]. In this study, *R. oryzae* was the dominant culturable fungus in all samples, followed by *A. fumigatus* and *A. flavus*. This finding agreed with some earlier reports that other fungi are associated with *R. oryzae* during barn rot in flue-cured tobacco [28, 29].

High-throughput sequencing showed that the Ascomycota was the dominant phylum followed by Basidiomycota and Mucoromycota. Ascomycota has been shown to be the most common phyllosphere fungi in many crops [30], but both Ascomycota and Basidiomycota were the dominant taxons isolated from tobacco leaves [31]. This is similar to this study. However, the taxons respond differently to the curing process. Ascomycota OTUs decreased greatly during curing, whereas Basidiomycota OTUs showed no significant changes during curing.

At a genus level, this study showed that the fungal OTUs were largely dominated by *Alternaria*, followed by *Phoma*, *Boeremia*, *Cladosporium*, *Aspergillus*, *Cercospora*, *Golovinomyces* and *Rhizopus*. In non-flue-cured and flue-cured tobacco leaves, the genera most frequently cultured, in decreasing frequency, were *Alternaria*, *Cladosporium*, *Epicoccum*, *Trichoderma*, *Nigrospora*, *Penicillium*, *Chaetomium*, *Fusarium* and *Aspergillus* [32-34]. Thus, this study showed a considerable overlap in the frequency of fungal genera previously reported from tobacco leaves with *Alternaria* consistently being the most dominant leaf fungus. The high frequency of *Alternaria* is not surprising as it includes 100 species distributed worldwide over various agroclimtic zones and ecosystems and includes many important saprophytic and phytopathogenic fungi. *Alternaria alternata* is a facultative necrotrophic fungus on tobacco tissues producing toxins causing tobacco brown spot disease that commonly occurs during leaf senescence [35]. In addition to detecting *Alternaria* OTUs, *A. alternata* was isolated from leaves in this study indicating that brown spot disease was occurring in the curing chamber in this study. Although several studies, such as Welty et al. [7, 33] have found culturable *Penicillium* species being dominant on flue-cured tobacco leaves, relatively few *Penicillium* OTUs and no *Penicillium* isolates were found in this study.

As all tobacco leaf samples were collected in a curing chamber where tobacco pole rot disease occurred, it was expected that *R. oryzae* would be detected as it is the causal agent of pole rot of tobacco [8, 36]. In this study, *Rhizopus* was detected from all samples by using both cultural-dependent method and high-throughput sequencing technique, and it was detected at all curing stages in both petioles and lamina and at all positions in the curing chamber. However, *Rhizopus* OTUs were most common in petiole during yellowing stage at the upper position, and least common in lamina during color fixing at the middle and lower position. Similarly, cultures of isolates of *R. oryzae* were most common during yellowing and stem-drying stages, and least common in color-fixing stage. Thus, it is common under these conditions but is affected by environmental and biological conditions. It was not surprising that it could be found in all curing stages as the fungus can survive at much high temperatures [37, 38] than those recorded in this study.

Previous studies showed that higher temperature and increased humidity favored pole rot disease development, and infection was usually first seen in the butts of leaves, which corresponds to the petiole tissue in this study [39, 40]. In this study, pole rot was more serious on leaves located near the upper position in the curing chamber compared to the middle and lower positions. Environmental monitoring in the study showed that position in the chamber affected temperature and humidity, and also affected fungal OTU composition, especially for *Rhizopus*. The other fungal OTUs in this study which showed the most similar impacts of the environment as *Rhizopus* were *Aspergillus*, *Pallidocercospora* and *Didymella*.

Using the FUNGuild database to assign fungal genera to functional guilds [41], most of the fungal OTUs in this study were identified as pathotroph-saprotroph-symbiotroph, followed by pathotroph-saprotroph and pathotroph. This indicated that a large number of the fungi on the tobacco phyllosphere during curing have potential plant pathogenic characteristics as well as many can be saprotrophs. This includes genera with species of known tobacco pathogens, such as the facultative necrotrophs, *A. alternata* that causes brown spot [8], *Phoma omnivirens* that causes black spot stalk [42] and *Cercospora nicotianae* that causes frogeye [43], as well as the

obligate biotroph, *Golovinomyces* that causes powdery mildew [44]. Most likely, these pathogens have arrived on tobacco leaves from diseased tissue in the field, and some could be growing both pathogenically inside the leaves as well as saprophytically on leaf surfaces during curing.

This study enlarges our knowledge of the fungal community of the tobacco phyllosphere on tobacco leaves during flue-curing. It showed that the environment during curing can impact fungal community composition and diversity, including fungal pathogens, such as those causing tobacco pole rot and brown spot. In addition to fungi, there are many bacteria associated with tobacco leaves, such as those able to cause leaf rot of tobacco [45]. More studies need to be conducted in this topic in the future. In this study, an air-rising curing chamber was used, but there are also air-falling chambers used for tobacco curing [46, 47]. It would interesting to learn if the two types of air flow systems would have different impact of microbial composition and diversity during tobacco leaf curing.

5. Conclusions

In conclusion, the obtained data from this study showed that the leaf fungal communities at yellowing, color-fixing and stem-drying stages were markedly different in terms of alpha and beta diversity. *Alternaria*, *Phoma*, *Boeremia*, *Cladosporium*, *Aspergillus*, *Cercospora*, *Golovinomyces* and *Rhizopus* were the main fungal OTUs in the curing chamber, and as curing progressed, humidity and temperature were the key environmental factors shaping the leaf fungal community. Understanding the dynamics of the fungal phyllosphere provide insights into selecting antagonistic microbes adapted to conditions of tobacco leaf curing that could provide new biocontrol of tobacco diseases, such as tobacco pole rot and brown spot during curing.

Declarations

Ethics approval and consent to participate

Not applicable.

Consent for publication

Not applicable.

Availability of data and material

The amplified fragments were sequenced, and all raw ITS gene sequence data is published under the NCBI (http://www.ncbi.nlm.nih.gov/)

Competing interests

The authors declare no competing financial interests.

Author contributions

Conceived and designed the experiments: H.C.W. Performed the experiments: Q.L.C., L.C., L.T.C. Analyzed the data: Q.L.C., and H.C.W. Wrote and revised the paper: Q.L.C., H.C.W., J.M. F.W., P.G. and Z.L.

References

1. Liu, L. P., Qu, J. W., Yi, X. Q., Huang, H. H. Genome-wide identification, classification and expression analysis of the mildew resistance locus o (MLO) gene family in sweet orange (citrus sinensis). Brazilian Archives of Biology and Technology. 2017; 60: 1678-4324.

2. Naidu, S. K. Tobacco: Production, Chemistry and Technology. Crop Science. 2001;41(1): 255.

3. Burton, H. R., Andersen, R. A., Fleming, P. D., Walton, L. R. Changes in chemical composition of burley tobacco during sensecence and curing. 2. acylated pyridine alkaloids. Journal of Agricultural & Food Chemistry. 1988; 36(3): 579-584.

4. Morin, A., Porter, A., Joly, J., Ratavicius, A. Evolution of tobacco-specific nitrosamines and microbial populations during flue-curing of tobacco under direct and indirect heating. Beiträge zur Tabakforschung International/Contributions to Tobacco Research. 2014. 21(1): 2013-0770.

5. Zheng, S., Wu, C., Bao, Y., Wang, Y. Influential parameters analysis on heating performance of heat pump in baking process. Procedia Engineering. 2017; 205(2017): 810-817.

6. Spurr, H. W. Bacterial barn rot of flue-cured tobacco in North Carolina. Plant Disease. 1980: 64(11), 1020.

7. Welty, R. E., Lucas, G. B. Fungi isolated from damaged flue-cured tobacco. Applied Microbiology. 1968;16(6): 851-854.

8. Wang, H. C., Huang, Y. F., Tang, X. G., Cai, L. T., Chen, Q. Y., Wang. M. S., Shang, S. H. Leaf and stem rot of tobacco (*Nicotiana tabacum* l.) caused by *Rhizopus oryzae* in closed curing barns in Guizhou province of china. Plant Disease. 2016; 100(2): 536.

9. Pan, Z. X., Cai, Y. Z., He, P. F. Isolation, identification and characterization of the pathogen of tobacco leaf mold during flue-curing. Acta Tabacaria Sinica. 2019;40(04): 42-47.

10. Kortekamp, A., Schmidtke, M., Serr, A. Infection and decay of tobacco caused by *Rhizopus oryzae* / Die Infektion und Fäulnis von Tabak verursacht durch *Rhizopus oryzae*. Journal of Plant Diseases and Protection. 2003; 110:535-543.

11. Gu, G., Xiao, S., Zhou, T., Liu, G. K., Wang, S. L., Zhang, S. S. Research progress and prospect of tobacco leaf mould rot during baking period. Acta Tabacaria Sinica. 2018; 24(05): 112-116.

12. Cai, L. T., Wang, H. C., Chen, Q. L., Tan, Q. Q., Yang, X. H., Ma, J. Sensitivity of *Rhizopus oryzae* to six fungicides and the screening of its preservation conditions. Chinese Journal of Pesticide Science. 2019; 21(4): 431-436.

13. Luo, L. Y., Zhang, Z., Wang, P, Han, Y. Q., Jin, D. C., Su, P, Tan, X. Q., Zhang, D. Y., Rizwan, H. M., Lu, X. Y., Liu, Y. Variations in phyllosphere microbial community along with the development of angular leaf-spot of cucumber. AMB Express. 2019; 9(1): 76.

14. Raza, M., Zhang, Z. F., Hyde, K. D., Diao, Y. Z., Cai, L. Culturable plant pathogenic fungi associated with sugarcane in southern china. Fungal diversity. 2019; 99(1): 1-104.

15. Chen, Q. L., Li, Zhong., Wang, H. C., Huang, Y., Cai, L. T., Xie, H. L., Zhou, H. Fungal composition and diversity of tobacco phyllosphere from cured tobacco leaves. Acta Microbiologica Sinica. 2019; 59(12): 2401-2409.

16. Liu, C., Wang, H. C., Xie, H. L., Xiang, L. G., Huang, Y., Chen, Q. L., Yu, Z. H., Zhou, G. J. Biodiversity analysis of phyllosphere bacterial genus from tobacco leaves infected by brown spot disease. Tobacco Science & Technology, 2019.

17. Xiang, L. G., Zhou, H., Wang, H. C., Li, Z., Chen, Q. L., Yu, Z. H. Bacterial community structure and diversity of *Rhizosphere* soil and stem of healthy and bacterial wilt tobacco plants. Acta Microbiologica Sinica. 2019; 59(10): 1984-1999.

18. Gong, J., Liu, Y. P., Li, Y. Y. Comparative analysis of microbial communities on tobacco leaves between clone library and high-throughput sequencing. Journal of East China Normal University. 2016; 2016(03): 92-101+114.

19. Chen, S. Y., Li, J. J., Lin, J., Bao, K. X., Fan, J. Q., Zhang, R. Q., Chen, Y. Q., Chen, S. B., He, W. High-throughput sequencing fungal community structures in aging tobacco strips from different growing areas and stalk positions. Tobacco Science & Technology. 2018; 51(04), 12-19.

20. Mboowa, G., Sserwadda, I., Amujal, M., Namatovu, N. Human genomic loci important in common infectious diseases: role of high-throughput sequencing and genome-wide association studies. Canadian Journal of Infectious Diseases and Medical Microbiology. 2018; 6010: 1-9.

21. Attitalla, I. H., Al-Ani, L. K. T., Nasib, M. A. Screening of fungi associatedwith commercial grains and animal feeds in Al-Bayda Governorate, Libya. World Applied Sciences Journal. 2010; 9(7): 746-756.

22. Xu, C. Y., Liang, X. Y., Hou, Y. P., Zhou, M. G. Effects of the Novel Fungicide Benzothiostrobin on *Sclerotinia sclerotiorum* in the Laboratory and on Sclerotinia stem Rot in Rape Fields. Plant Disease. 2015; 99(7): 969-975.

23. Lv, D., Ma, A. Z., Tang, X. M., Bai, Z. H., Qi, H. Y., Zhuang, G. Q. Profile of the culturable microbiome capable of producing acyl-homoserine lactone in the tobacco phyllosphere. Journal of Environmental Sciences. 2013; 25(2): 357-366.

24. Lei, Y., Xiao, Y., Li, L. Impact of tillage practices on soil bacterial diversity and composition under the tobacco-rice rotation in China. Journal of Microbiology. 2017; 55(5): 349-356.

25. Hugenholtz, P. Exploring prokaryotic diversity in the genomic era. Genome Biology. 2002; 3(2): 1-8.

26. Ma, X., Jiang, M., Liu, J. Preliminary analysis of amplicon high-throughput sequencing as a method for the assessment of fungal diversity in discolored wood. Holzforschung. 2017; 71(10): 793-800.

27. Li, W. H., Jin, D. C., Shi, C. H. Midgut bacteria in deltamethrin-resistant, deltamethrin-susceptible, and field-caught populations of *Plutella xylostella*, and phenomics of the predominant midgut bacterium *Enterococcus mundtii*. Scientific Reports. 2018: 8(1),4991.

28. Cole, J. S. Fungicide control of barn rot of flue-cured tobacco caused by *Rhizopus arrhizus*. Rhodesian Journal of Agricultural Research. 1975; 13(1): 15-20.

29. Zeng, T. Y., Gu, G., Zhang, S. S. Identification of tobacco mildew pathogen which causes leaf rot during flue-curing. Acta Tabacaria Sinica. 2014; 20(4): 65-68.

30.

31. Angelini, P., Rubini, A., Gigante D. The endophytic fungal communities associated with the leaves and roots of the common reed (*Phragmites australis*) in Lake Trasimeno (Perugia, Italy) in declining and healthy stands. Fungal Ecology. 2012; 5(6):683-693.

32. Wu, K., Luo, H. Y., Lin, K. Fungi species in mildew tobacco leaves identified based on rDNA-ITS. Guizhou Agricultural Sciences. 2014; 42(06): 98-100.

33. Harvey, W. S. Bacterial barn rot of flue-cured tobacco in North Carolina. Plant Disease. 1980: 64(11),120.

34. Welty, R. E., Lucas, G. B., Fungi isolated from flue-cured tobacco at time of sale and after storage. Applied Microbiology. 1969; 17(3): 360-365.

35. Nagrale, D. T., Lalan, S., Sunil, K. Recent diagnostics and detection tools: implications for plant pathogenic *Alternaria* and their disease management. Springer International Publishing. 2016.

36. Duan, W. J., Zhang, X. Q., Yang, T. Z. A novel role of ammonia in appressorium formation of *Alternaria alternata* (Fries) Keissler, a tobacco pathogenic fungus. Journal of Plant Diseases and Protection. 2010; 117(3): 112-116.

37. Peng, Q. Y., Yi, T. Y. Analysis of tobacco mildew and its control measures. Chinese Agricultural Science Bulletin. 2007; 2007(11): 146-150.

38. Wickes, B. L. *Rhizopus oryzae*: Genetic Secrets of an Emerging Human Pathogen. Genomics of Soil- and Plant-Associated Fungi. Springer Berlin Heidelberg. 2013.

39. Gayed, S. K. *Rhizopus arrhizus* causing ploe rot of flue-cured tobacco in ontario. Canadian Journal of Plant Science. 1972; 52(1): 103-106.1

40. Paddick, R. G., Turner, P. L. Control of *Rhizopus* barn rot of flue-cured tobacco using dicloran. Australian Journal of Experimental Agriculture. 1973; 13(64): 612-615.

41. Deng, Y. L., Cui, G. M., Kong, G. H., Li, Z. J. Effect of variety, leaf position, and degree of maturity on starch content, flavor and taste of tobacco leaf. Chinese Tobacco Science. 2006; 27(4): 18-23.

42. Nguyen, N. H., Song, Z., Bates, S. T., Branco, S., Tedersoo, L., Menke, J. Funguild: an open annotation tool for parsing fungal community datasets by ecological guild. Fungal Ecology. 2016; 20(06): 241-248.

43. Jiang, Y., Sang, W. J., Zeng, E. L., Wang, Y., Wang, D. F., Qin, K. Identification of pathogenic fungus causing tobacco black spot stalk in Guizhou Province. Jiangs u Agricultural Sciences. 2018; 46(10): 92-95.

44. Fajola, A. O., Alasoadura, S. O. Chemical control of the frog-eye disease (*Cercospora nicotianae*) of tobacco (*Nicotiana tabacum*) in Nigeria. Annals of Applied Biology. 1973; 74(2): 219-224.

45. Mara, Q. L., Mario, F., Antonio, Z., Claudia, Z. Role of pathogen-induced volatiles in the *Nicotiana tabacum - Golovinomyces cichoracearum* interaction. Plant Physiology and Biochemistry. 2012; 52: 9-20.

46. Spurr, H. W. Bacterial barn rot of flue-cured tobacco in North Carolina. Plant Disease. 1980; 64(11): 1020.

47. Ngoni, C. C., Daniel, J., Peter, R., Zvirevo, C., Courage, B. Development of an efficient low-cost emergency tobacco curing barn for small scale tobacco growers in ZIMBABWE. Journal of Basic and Applied Research International. 2017; 20(4): 244-256.

48. He, X., Li, J. C., Hu, J., Cao, J. C. The effect of different air flow forms on the temperature and air distribution in bulk tobacco barn. Machinery Design & Manufacture. 2017; 2017(01):123-126.

Tables

Table 1. Environmental conditions for the tobacco samples collected from curing chamber

Period（h）	Sample name	Chamber position (m)	Air relative humidity (%)	Air temperature (℃)	Wind speed（r/min）	Petiole wetness (%)	Lamina wetness (%)	Lamina temperature (℃)
Yellowing （42）	A11-B11	(2.5)	91.5	37	960	78	67	35
	A12-B12	(1.75)	87.5	37.5	960	75	65	35.5
	A13-B13	(1)	84	38	960	73	63	36
Color-fixing（94）	A21-B21	(2.5)	73	47	1450	55	49	45
	A22-B22	(1.75)	66	47.5	1450	48	43	45.5
	A23-B23	(1)	57	48	1450	40	35	46
Stem-drying（140）	A31-B31	(2.5)	22	67	960	20	14	65
	A32-B32	(1.75)	12.5	67.5	960	11	8	65.5
	A33-B33	1	8.5	68	960	5	4	66

Table 2. Molecular identification of the total leaf fungi isolated from tobacco petioles and lamina in the baking chamber where tobacco pole rot occurred

Stages	Media	No. of Species	Species	Strain code (GenBank No.)	Leaf-position		Curing - position		
					Petiole	Lamina	Up	Middle	Lower
Yellowing	AEA	3	*Rhizopus oryzae*	AA111(MN010558), AA112(MN010559), AB111(MN006416), AA121(MN010561), AA122(MN010562), AA123(MN013932), AB121(MN013934), AB122(MN006419), AB123(MN006420), AA131(MN010563), AA132(MN013933), AB132(MN006423), AB133(MN006424),	6	7	3	6	4
			Aspergillus fumigatus	AA113(MN010560), AB131(MN006422)	1	1	1	0	1
			Aspergillus flavus	AB112(MN006417), AB113(MN006418), AA133(MN010564)	1	2	2	0	1
	PDA	3	*Rhizopus oryzae*	PA122(MN010551), PA131(MN010553), PA132(MN010554), PA133(MN010555), PA111(MN010548), PA112(MN010549), PA113(MN013935), PB112(MN006654), PA123(MN010552), PB121(MN006656), PB122(MN006657), PB123(MN013936), PB131(MN010536), PB132(MN010537), PB133(MN010538),	8	7	4	5	6
			Aspergillus fumigatus	PB111(MN006653), PB113(MN006655)	0	2	2	0	0
			Aspergillus flavus	AA133(MN010564)	1	0	0	0	1
Color-fixing	AEA	5	*Rhizopus oryzae*	AB211(MN006425), AB223(MN006430), AB233(MN006433), AA232(MN006405),	1	3	1	1	2
			Epicoccum sorghinum	AB231(MN006431), AB232(MN006432)	0	2	0	0	2
			Cladosporium tenuissimum	AA212(MN010566), AB212(MN006426)	1	1	2	0	0
			Aspergillus fumigatus	AA231(MN006404), AA233(MN006406), AA211(MN010565), AB213(MN006427)	3	1	2	0	2
			Aspergillus flavus	AB221(MN006428), AB222(MN006429), AA213(MN006400) AA221(MN006401), AA222(MN006402), AA223(MN006403)	4	2	1	5	0
	PDA	8	*Rhizopus oryzae*	PB232(MN010546)	0	1	0	0	1
			Epicoccum thailandicum	PB231(MN010545)	0	1	0	0	1
			Diaporthe ovalispora	PA231(MN006635)	1	0	0	0	1
			Aspergillus oryzae	PB211(MN010539)	0	1	1	0	0
			Aspergillus fumigatus	PA232(MN006636), PA212(MN010557), PA221(MN006632), PB233(MN010547)	3	1	1	1	2
			Aspergillus flavus	PA211(MN010556), PA213(MN006631), PB213(MN010541), PA222(MN006633), PA223(MN006634), PB221(MN010542), PB222(MN010543), PA233(MN006637)	5	3	3	4	1
			Aspergillus aflatoxiformans	PB223(MN010544)	0	1	0	1	0
			Alternaria alternata	PB212(MN010540)	0	1	1	0	0
Stem-dring	AEA	1	*Rhizopus oryzae*	AA312(MN006408), AA313(MN006409), AB311(MK988567), AB312(MK988568), AB313(MK988569), AA322(MN006411), AA323(MN006412), AB321(MK988570), AB322(MK988571), AB323(MN006434), AA331(MN006413), AA332(MN006414), AA333(MN006415), AA321(MN006410), AB331(MN006435), AB332(MN006436), AB333(MN006437), AA311(MN006407),	9	9	6	6	6
	PDA	2	*Rhizopus oryzae*	PA311(MN006638), PA312(MN006639), PA313(MN006640), PB313(MN006667),PA321(MN006647), PA322(MN006648), PA323(MN006649), PA331(MN006650), PA332(MN006651), PA333(MN006652), PB311(MN006665), PB312(MN006666), PB321(MN006668), PB323(MN006670), PB331(MN006671), PB332(MN006672), PB333(MN006673),	9	8	6	5	6
			Aspergillus flavus	PB322(MN006669)	0	1	0	1	0

Table 3. Alpha- diversity indexes of fungal community and OTU numbers based on high-throughput sequencing in different samples

Stage	Position	Sample	Petiole					Sample	Lamina				
			Shannon	Simpson	Chao1	ACE	OTU		Shannon	Simpson	Chao1	ACE	OTU
Yellowing	Up	A11	5.17±0.77	0.92±0.04	549±58	557±60	564±66	B11	6.35±0.06	0.96±0.00	708±45	707±50	714±51
	Middle	A12	5.42±0.17	0.91±0.01	643±27	644±23	634±16	B12	5.50±0.84	0.91±0.69	614±49	620±48	622±67
	Lower	A13	5.07±0.73	0.86±0.08	623±21	639±20	644±34	B13	4.96±0.64	0.88±0.07	561±58	567±51	568±50
	Average		5.22±0.63	0.90±0.06	604±56	614±56	608±72		5.60±0.83	0.92±0.07	628±79	613±76.	635±83
Color-fixing	Up	A21	3.24±1.04	0.61±0.20	522±72	540±73	537±71	B21	5.44±0.64	0.90±0.08	678±3	682±6	695±6
	Middle	A22	6.63±0.33	0.97±0.01	729±18	732±18	717±35	B22	6.19±0.28	0.96±0.02	696±24	707±25	717±16
	Lower	A23	6.35±0.05	0.97±0.00	675±31	674±28	678±31	B23	5.66±0.55	0.95±0.02	622±122	632±118	645±117
	Average		5.40±1.66	0.85±0.20	642±99	649±93	644±92		5.67±0.60	0.93±0.50	666±78	673±76	686±75
Stem-dring	Up	A31	5.75±0.45	0.93±0.04	715±82	729±79	745±74	B31	5.63±0.13	0.92±0.02	730±16	740±14	736±20
	Middle	A32	6.39±0.11	0.97±0.00	748±2	760±5	759±19	B32	6.65±0.19	0.97±0.00	737±38	737±35	749±25
	Lower	A33	6.34±0.15	0.95±0.01	821±80	823±77	824±73	B33	6.89±0.15	0.98±0.01	855±31	862±31	879±33
	Average		6.16±0.40	0.95±0.03	761±80	771±75	776±70		6.39±0.57	0.96±0.03	774±65	780±65	788±70
Total			5.60±1.10	0.90±0.12	670±102	678±100	676±106		5.92±0.75	0.94±0.53	689±95	695±94	703±99

Note: Richness and diversity estimation of the ITS sequencing libraries from the sequencing analysis. Shannon and Simpson are used to assess the community diversity, while Chao and Ace are used to evaluate the community richness. The values of mean ± SD of Three samples are shown in the table.

Table 4. The top10 dominant taxa and their relative abundance of fungal community of sample (Relative abundance %)

| Stages	Leaf-position	Samples	Alternaria	Phoma	Boeremia	Cladosporium	Aspergillus	Cercospora	Golovinomyces	Rhizopus	Symmetrospora	Golubevia
Yellowing	Petiole	A11	20.80%	11.91%	0.23%	0.61%	16.33%	4.65%	0.01%	5.54%	0.63%	0.09%
		A12	23.56%	15.36%	1.27%	0.89%	2.95%	3.18%	0.04%	0.07%	3.98%	0.34%
		A13	8.55%	9.49%	2.70%	24.17%	1.14%	0.70%	0.04%	0.03%	0.86%	0.03%
	Lamina	B11	7.81%	15.24%	0.63%	1.33%	1.17%	8.50%	0.01%	0.30%	3.43%	0.11%
		B12	9.74%	12.26%	19.31%	1.39%	5.31%	3.78%	0.00%	0.04%	2.85%	0.09%
		B13	15.62%	23.24%	3.88%	8.80%	2.64%	0.41%	0.03%	0.05%	0.25%	0.02%
Color-fixing	Petiole	A21	59.59%	2.11%	0.24%	0.53%	7.07%	1.32%	0.02%	0.34%	0.61%	0.32%
		A22	4.17%	6.43%	2.40%	3.06%	2.31%	11.89%	1.42%	0.45%	4.91%	0.17%
		A23	3.81%	7.93%	2.48%	4.15%	0.18%	5.66%	0.06%	0.01%	5.94%	0.28%
	Lamina	B21	28.27%	12.88%	0.84%	1.92%	0.71%	7.46%	0.02%	0.10%	2.24%	5.55%
		B22	1.60%	6.81%	1.41%	2.07%	0.21%	15.35%	6.73%	0.00%	3.80%	0.08%
		B23	6.61%	5.78%	8.44%	6.08%	0.14%	4.46%	0.03%	0.00%	2.75%	0.10%
Stem-drying	Petiole	A31	14.14%	3.24%	0.46%	1.13%	5.86%	8.35%	1.87%	1.22%	3.00%	2.30%
		A32	4.45%	6.99%	0.43%	4.60%	17.94%	4.48%	0.06%	0.72%	2.17%	0.18%
		A33	1.30%	1.64%	0.40%	2.51%	4.94%	3.64%	0.80%	0.26%	2.91%	1.26%
	Lamina	B31	5.90%	7.61%	0.21%	4.24%	0.73%	16.46%	0.28%	0.03%	3.20%	4.58%
		B32	2.57%	9.54%	3.09%	4.15%	12.11%	4.80%	0.06%	1.60%	3.07%	0.10%
		B33	4.44%	8.66%	0.37%	3.26%	0.49%	7.27%	0.18%	0.05%	4.42%	0.43%
Total			12.38%	9.28%	2.71%	4.16%	4.57%	6.24%	0.65%	0.60%	2.84%	0.89%

Figures
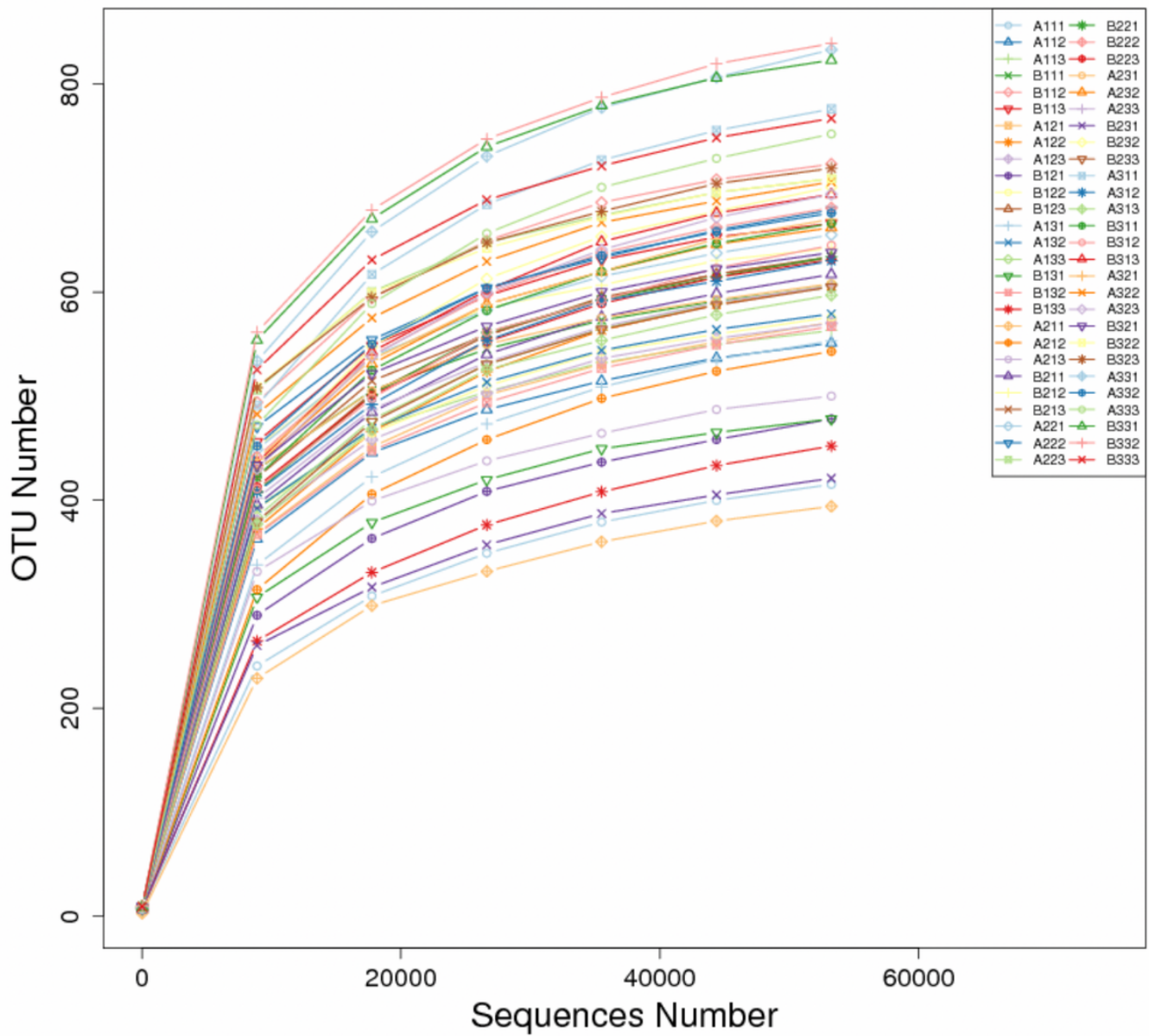
Figure 1

Rarefaction curves of OTUs across different tobacco leaf samples
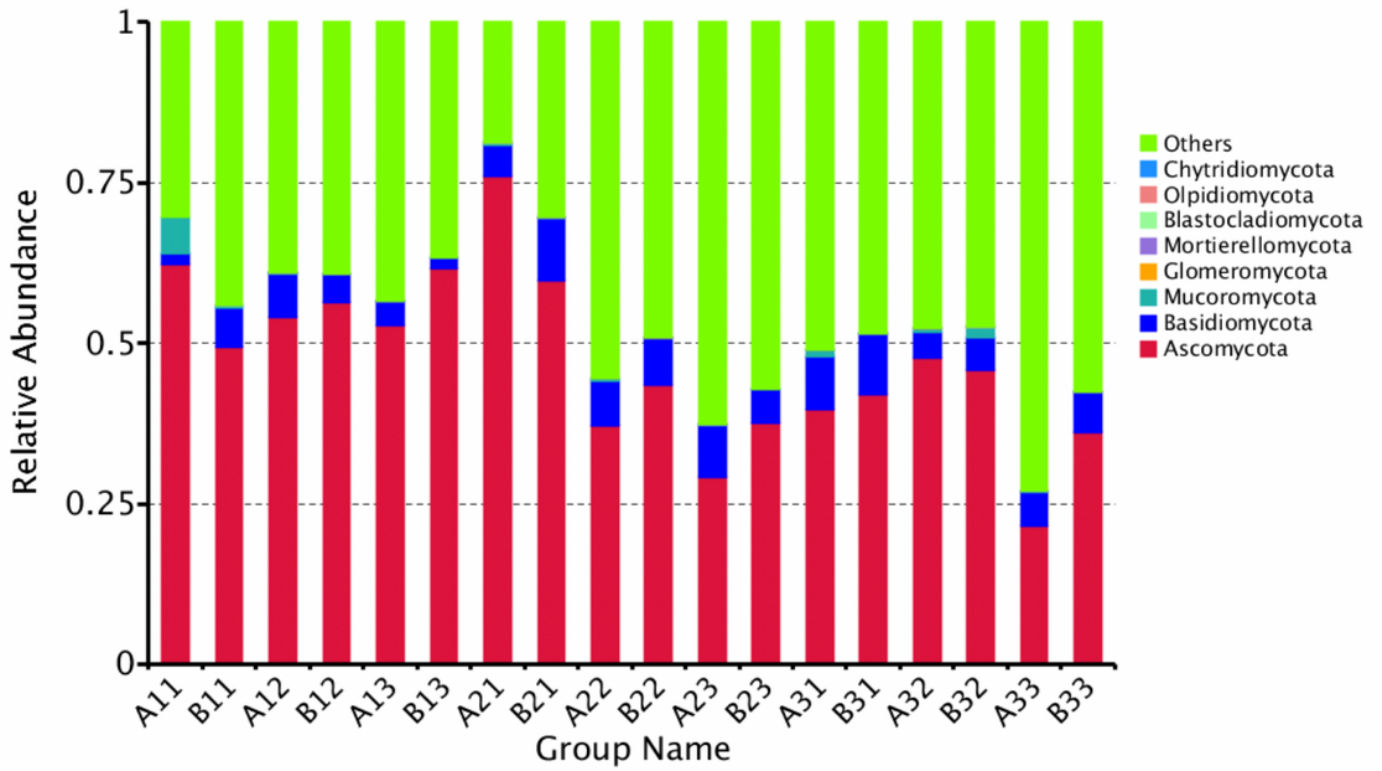
Figure 2

The relative abundance of different samples at Phylum level. Abundances of different bacterial phyla in the eighteen samples. The abundance was presented in terms of percentage among the total effective fungus sequences in each sample. The top ten abound taxa were shown.
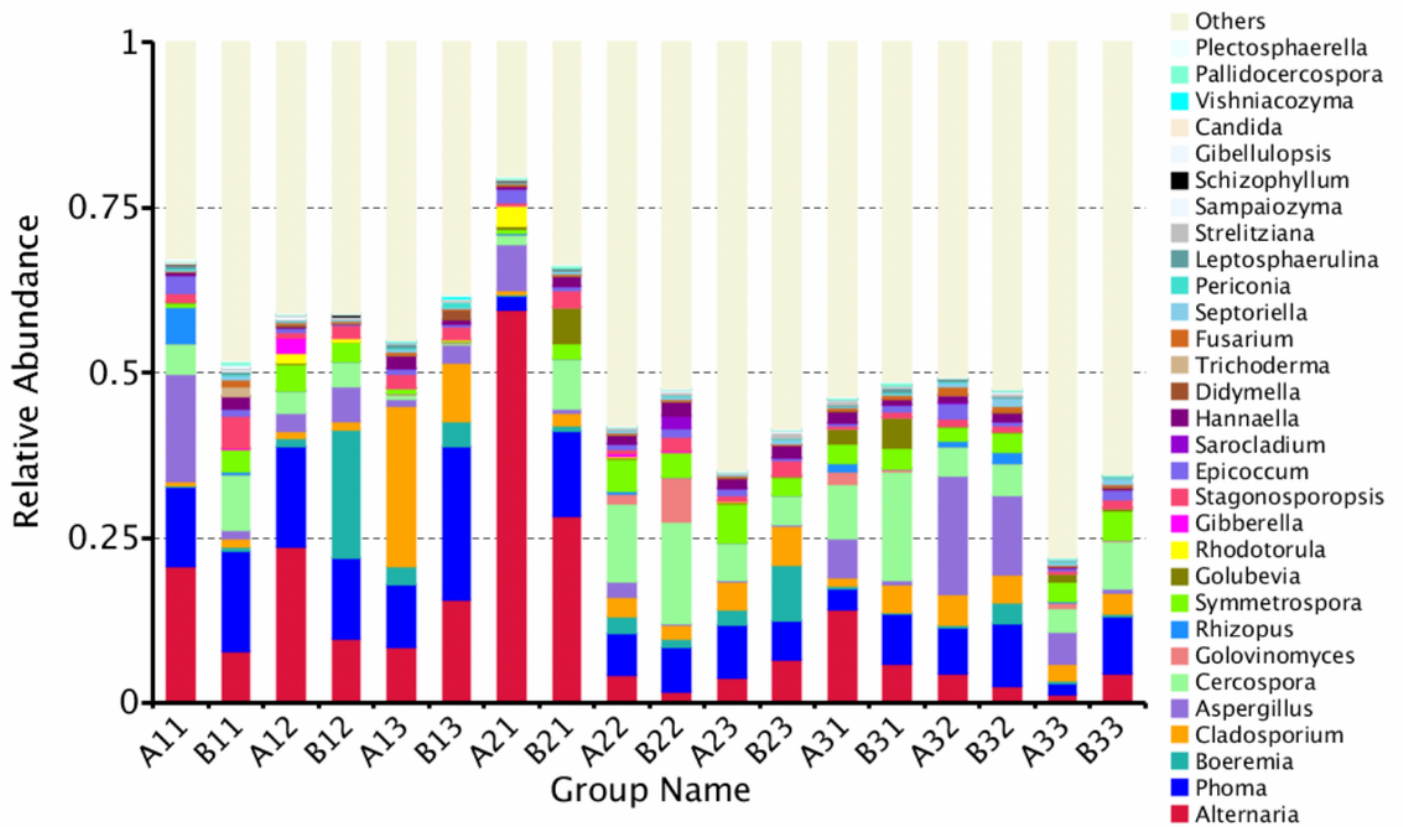
Figure 3

The relative abundance of different samples at genus level Abundances of different bacterial genus in the eighteen samples. The abundance was presented in terms of percentage among the total effective fungus sequences in each sample. The top thirty abound taxa were shown.

Figure 4

Maximum likelihood tree of 100 most abundant fungal genera in the Eighteen groups samples from the flue-cured tobacco obtained by analysis of ITS rDNA pyrosequencing data. Pink and Blue parts of the color range represented the genera of Ascomycota and Basidiomycota, respectively. A color-coded bar plot showed the distribution of each fungal genus in different samples.
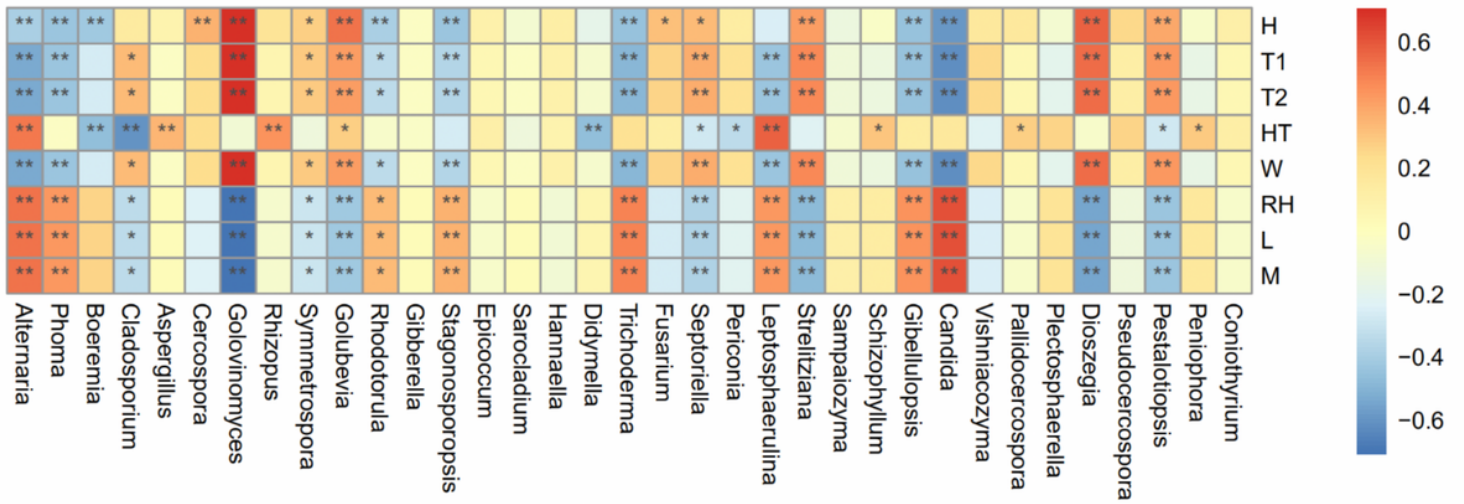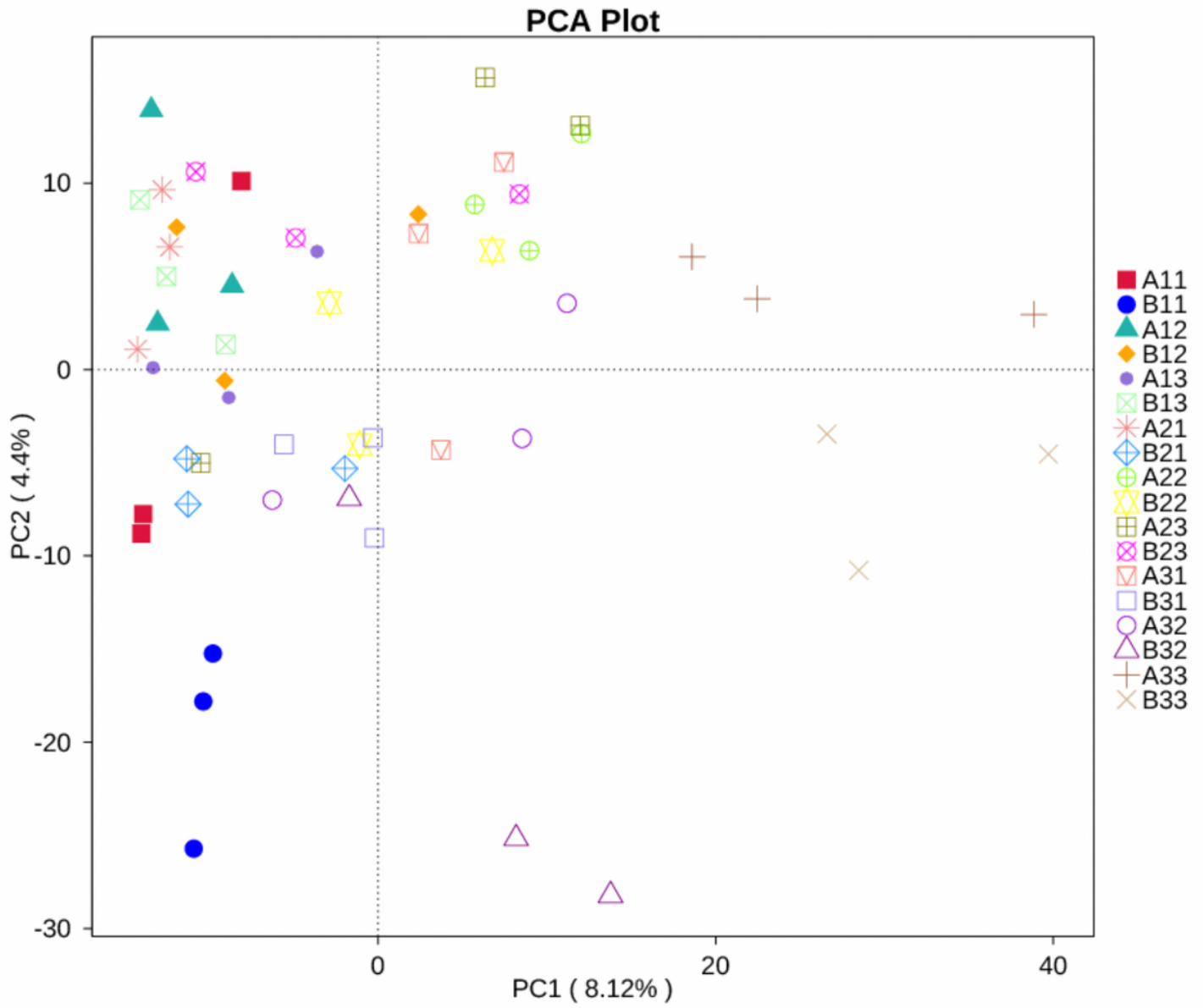
Figure 5

Spearman correlation analysis heatmap. Spearman's correlations between major genus and environmental factor relative abundances. Baking time (hour, H), air temperature (T1), petiole or lamina temperature (T2), height of tobacco hanging (Height, HT), wind speed (Wind, W), air relative humidity (RH), lamina wetness (LRWC, L) and petiole wetness (MVWC, M). "*" and "**" indicated p < 0.05 and p < 0.01, respectively.

Figure 6

Principal Component Analysis (PCA) analysis of the fungal communities in the 18 groups samples.
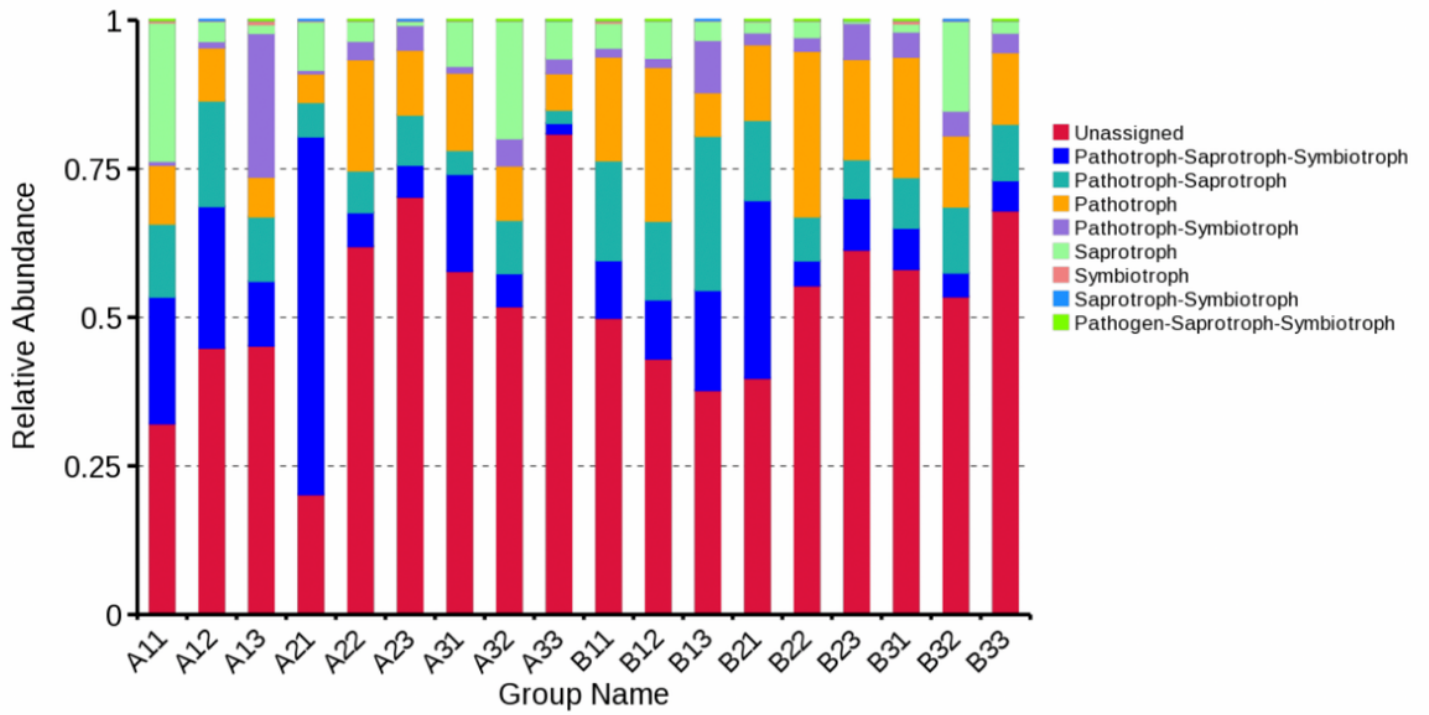
Figure 7

Relative abundance of fungal functional groups (guilds) based on OTU annotation table with disturbance frequency level.